Journal of Alloys and Compounds, 207/208 (1994) 449–453
JALCOM 3089

Thermodynamic assessment of Fe–Tb and Fe–Dy phase diagrams and prediction of Fe–Tb–Dy phase diagram

Susanne Landin and John Ågren
Department of Materials Science and Engineering, Royal Institute of Technology, S-100 44 Stockholm (Sweden)

Abstract

The Fe–Tb and Fe–Dy systems are assessed by means of the CALPHAD technique and thermodynamic descriptions of the individual phases are obtained. The two binaries are combined assuming ideal solution between Tb and Dy and the full ternary system Fe–Tb–Dy is calculated. The compounds are approximated as stoichiometric on the binary side and line compounds in the ternary system and their enthalpies are estimated from measurements in the Fe–Gd system. A satisfactory agreement is found between a calculated vertical section and the corresponding experimental information.

1. Introduction

Recently much attention has been paid to Fe–Tb–Dy alloys due to their giant magnetostriction related to the occurrence of a Laves phase. In spite of their interesting properties, ternary phase diagram information is almost completely missing. Such information should be a most valuable tool in the design of new magnetostrictive materials and the present study was performed in an attempt to rationalize the rather sparse experimental information by means of a thermodynamic approach denoted as the CALPHAD technique.

2. Experimental data

The experimental information is very sparse and concerns only the binary Fe–Tb and Fe–Dy phase diagrams and a vertical section in the ternary system. No thermochemical measurements have been reported except the enthalpy of formation for the Laves phase Fe_2R, where R stands for Dy or Tb (see Section 3). Dariel *et al.* [1] investigated the Fe–Tb system by means of metallography, X-ray diffraction, differential thermal analysis (DTA) and electron microprobe analysis. The Fe–Dy system was investigated by van der Goot and Buschow [2] who applied X-ray diffraction, metallography and thermal analyses in the range of 26–100 at.% Fe. A peritectoid reaction to the solid $Fe_{23}Dy_6$ was assumed in the Fe–Dy system rather than the peritectic transformation suggested in the hand drawn diagram by Van Der Goot and Buschow [2]. A eutectic or peritectic transformation would require a very unsymmetric liquidus curve for Fe_3Dy indicating an anomalous thermodynamic behavior of the liquid. Such a behavior seems less likely. A vertical section of the ternary Fe–Dy–Tb system at a constant Tb to Dy ratio, $Tb_{0.27}Dy_{0.73}Fe_x$, with $x = 0.8$–3.0, was examined by means of DTA, X-ray diffraction and metallography by Westwood and Abell [4].

3. Enthalpy of formation for intermediate phases

Iron and rare earth metals form several intermediate phases, *i.e.* Fe_2R, Fe_3R, $Fe_{23}R_6$ and $Fe_{17}R_2$, where R–Tb or Dy or both. Dehodar and Ficalora [5] measured the enthalpy of formation of Fe_2R. However, their measurements yielded a much higher stability for Fe_2Dy and Fe_2Tb than expected from the general tendency observed for transition metal rare earth compounds reported by Colinet and Pasturel [6]. The value reported by Dehodar and Ficalora [5] is around 30 times larger than the expected value by Colinet and Pasturel [6] and 7 times larger than that predicted by the Miedema method [7]. As such a large difference is difficult to explain, it was decided not to take these measurements into account. On the other hand, Colinet and Pasturel [8] have measured the enthalpies of formation of all the intermediate phases in the Fe–Gd system and found that the enthalpy of formation of Fe_2Gd is about twice as much negative as the value predicted by Miedema [7]. It seems reasonable to believe that the intermediate phases in the Fe–Dy, Fe–Tb and Fe–Gd systems would

SSDI 0925-8388(93)03089-2

be very similar and due to the lack of experimental data, we have simply assumed the same numbers on the enthalpies of formation at 298.16 K for the intermediate phases in Fe–Dy and Fe–Tb. Upon further examination of the melting point of the Laves phases in the different lanthanide systems [9], one would expect Fe_2Tb and Fe_2Dy to be slightly more stable than Fe_2Gd. Some information [1,10] indicates that at least Fe_2R has a homogeneity range at high temperatures but due to lack of more precise data, it was approximated as stoichiometric at all temperatures. The present prediction was made by comparing the stabilities.

4. Thermodynamic models

The molar Gibbs energy of formation for the various phases is represented by expressions of the type:

$$^{\circ}G_{A_mB_n} = m\,^{\circ}G_A + n\,^{\circ}G_B + A + BT \quad (1)$$

It is thus assumed that the Neumann–Kopp rule applies to the heat capacity. All $^{\circ}G$ values are given relative to the enthalpy of the elements at 298.16 K and their entropy at 0 K. This reference is denoted by SER, stable element reference [11]. As mentioned, all the intermediate phases are treated as stoichiometric on the binary sides with Fe on one sublattice and the R-component on the other. In the ternary system, it is assumed that Tb and Dy form an ideal solution on the second sublattice. The molten metal is treated as a regular solution without any ternary interaction. Moreover, due to lack of data and similar properties, Tb and Dy are assumed to form ideal solutions both in the solid and liquid phases.

5. Lattice stabilities

Tb and Dy only exist in the HCP and the BCC crystal structures [12]. In the assessment of the binaries, the lattice stabilities of the hypothetical FCC states are needed. These values have not been reported but are estimated rather arbitrarily as

$$^{\circ}G_{Dy}^{FCC} = {}^{\circ}G_{Dy}^{HCP} + 5000 \quad (2)$$

$$^{\circ}G_{Tb}^{FCC} = {}^{\circ}G_{Tb}^{HCP} + 5000 \quad (3)$$

This choice guarantees that the FCC phase will not appear in the Tb–Dy system.

6. Optimization

The unknown thermodynamic parameters, *i.e.* the two regular solution parameters of Fe–Tb and Fe–Dy liquids, and the Gibbs energy of formation for all the intermediate phases, assuming a linear temperature dependence, were evaluated by a least square fit to all the experimental data and the enthalpies of formation at 298 K for the intermediate phases, estimated from the Fe–Gd system (see Section 3). The optimization was made using the PARROT program [13]. The two binary systems were optimized one at a time. Due to lack of data, the solubility of Fe in Tb and Dy was not taken into account, although some solubility should be expected. The present optimization is valid down to about 800 K, where the magnetic contribution to the Gibbs energy of the intermediate phases is negligible. An attempt was made to consider also the magnetic effects in the assessment but there are no heat capacity measurements available above 300 K and the experimental information thus is too sparse to evaluate any magnetic contribution.

7. Results

7.1. Dy–Tb

As mentioned, the Dy–Tb system was assumed ideal. This is in accordance with the predictions by Gschneidner [3], who concluded complete miscibility between Dy and Tb by studying systematics of the intra-lanthanoid binaries. This assumption is further supported by lattice parameter measurements by Gschneidner and Calderwood [14].

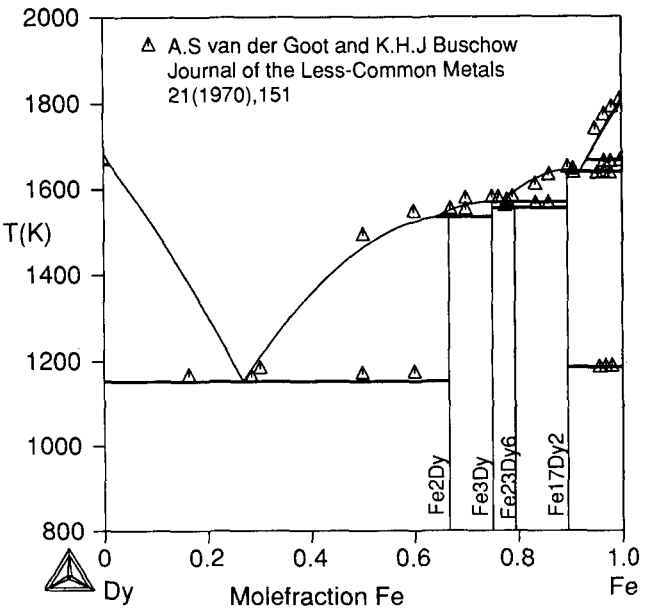

Fig. 1. The assessed Fe–Dy equilibrium phase diagram. Symbols: measurements by van der Goot and Buschow [2].

7.2. Fe–Dy

The calculated phase diagram is in good agreement with the experiments reported by Van Der Goot and Buschow [2] (see Fig. 1). A major difference with their hand drawn diagram is that the $Fe_{23}Dy_6$ phase forms by a peritectoid reaction just a few degrees below the eutectic $L \rightarrow Fe_3Dy + Fe_{17}Dy_2$ instead of the reactions $L + Fe_{17}Dy_2 \rightarrow Fe_{23}Dy_6$ and $L \rightarrow Fe_{23}Dy_6 + Fe_3Dy$ (see Fig. 2).

7.3. Fe–Tb

The calculated phase diagram is in good agreement with the measurements of Dariel *et al.* [1] (Fig.3).

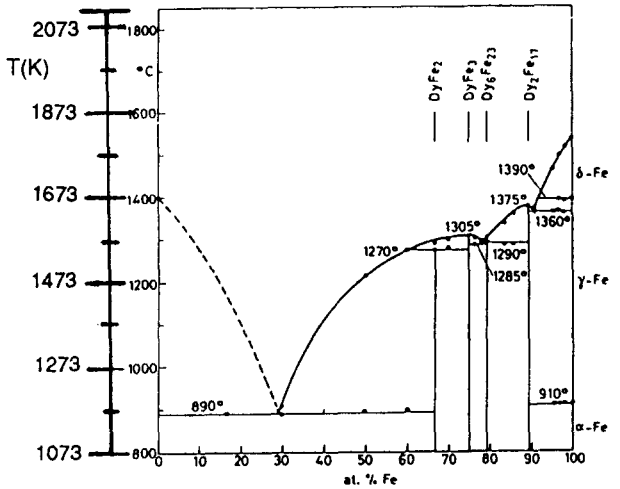

Fig. 2. The Fe–Dy phase diagram as drawn by van der Goot and Buschow.

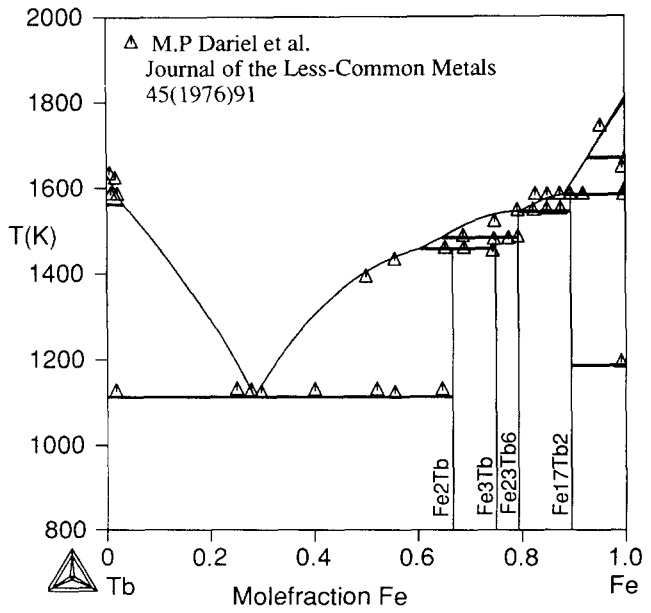

Fig. 3. The assessed Fe–Tb equilibrium phase diagram. Symbols: measurements by Dariel *et al.* [1].

7.4. Fe–Tb–Dy

The calculated diagram, obtained by combining the descriptions of the three binaries, is a prediction because no ternary information was included in the optimization. Consequently, there are no ternary interaction parameters. All the intermediate phases in the Fe–Tb phase diagram also appear in the Fe–Dy diagram. In a projection along the temperature axis, we thus have four lines crossing the ternary (see Fig. 4). As mentioned, Westwood *et al.* [4] reported a vertical section represented by the formula $Tb_{0.27}Dy_{0.73}Fe_x$ ($x = 0.8$–3.0). The calculated section agrees fairly well with their experimental section (see Fig. 5). One discrepancy is

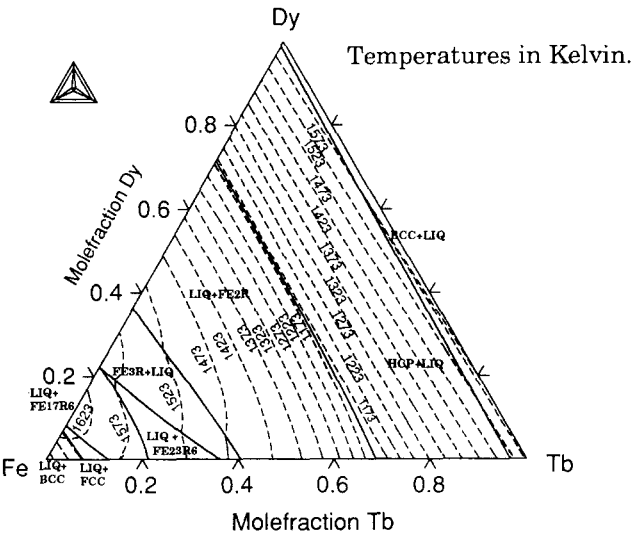

Fig. 4. Calculated liquidus surface of the calculated ternary Fe–Dy–Tb phase diagram. The dashed lines are isotherms and the full lines indicate three phase equilibria involving the liquid.

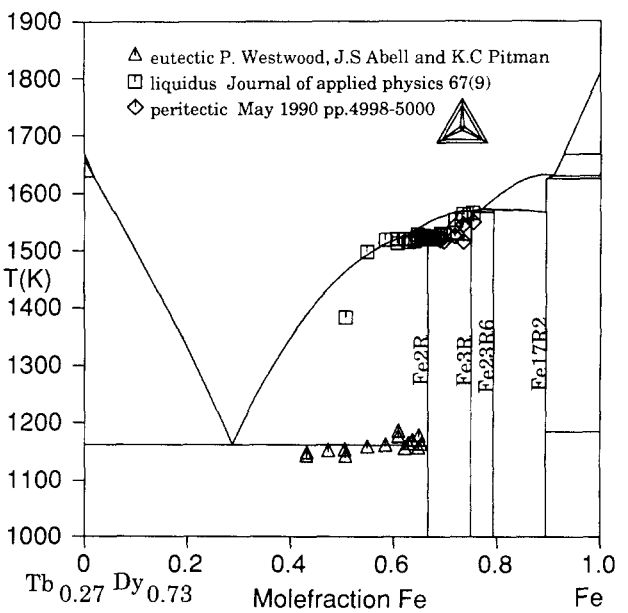

Fig. 5. Calculated vertical section, ($Tb_{0.27}Dy_{0.73}Fe_x$). Symbols: measurements by Westwood *et al.* [4].

that the liquid is more stable at high temperatures and less stable at low temperatures, 1300–1150 K according to the experimental information. However, such a shape of the liquidus surface is difficult to reconcile with information on the binaries, *i.e.* Figs. 1 and 3.

8. Conclusions

The ternary phase diagram Fe–Tb–Dy is calculated by means of the CALPHAD method. Satisfactory agreement with the sparse experimental information is found. A thermodynamic description of the individual phases has been obtained and arbitrary sections of the phase diagram may now be calculated. The present description should be a most useful starting point for further studies of phase equilibria in these systems. In particular, more precise experimental data on the extension of the intermediate phases is needed.

Acknowledgments

The authors want to express their gratitude to Dr. Bo Sundman and Dr. Armando Fernandez-Guillermet for valuable help and stimulating discussions. The present work is supported by the Swedish National Board for Industrial and Technical Development, NUTEK, and the Swedish Natural Science Research Council, NFR, and The Swedish council for planning and coordination of research, FRN.

References

1 M.P. Dariel, J.T. Holthuis and M.R. Pickus, *J. Less-Common Met., 46* (1976) 91.
2 A.S. Van der Goot and K.H.J. Buschow, *J. Less-Common Met., 21* (1970) 161.
3 K.A. Gschneider Jr., *J. Less-Common Met., 114* (1986) 29.
4 P. Westwood and J.S. Abell, *J. Appl. Phys., 67* (1990) 4998.
5 S.S. Dehodar and P.J. Ficalora, *High Temp. Sci., 8* (1976) 186.
6 C. Colinet and A. Pasturel, *CALPHAD, 11* (1987) 336.
7 A.K. Niessen, F.R. de Boer, R. Boom, de Chatel, W.C.M. Mattens and A.R. Miedema, *CALPHAD, 7* (1983) 61.
8 C. Colinet and A. Pasturel, *Met. Trans. A, 18A* (1987) 903.
9 S. Landin, unpublished.
10 J.S. Abell and D.G. Lord, *J. Less-Common Met., 126* (1986) 107.
11 I. Ansara and B. Sundman, *SGTE, Proc. Conf. CODATA*, Ottawa, Canada, 1987, p. 164.
12 A. Dinsdale, *CALPHAD, 16* (1991) 317.
13 B. Jansson, *TRITA-MAC 234*, Royal Institute of Technology, Stockholm, Sweden.
14 K.A. Gschneider Jr. and F.W. Calderwood, *Bull. Alloy Phase Diagrams, 4* (1983) 129.

Appendix

(1) *Liquid*

$^{\circ}G_{Dy}^{Liquid} - H_{Dy}^{SER}$

$298.15 < T < 1000$: $4010.058 + 124.111866T - 31.3602T\ \ln(T) + 6.14295 \times 10^{-3}\ T^2 - 2.123617 \times 10^{-6} T^3 + 31704T^{-1}$

$1000 < T < 1659$: $292367.773 - 2487.67879T + 337.520022T\ \ln(T) - 0.197339631T^2 + 1.800701 \times 10^{-5} T^3 - 41317706T^{-1}$

$1659 < T < 3000$: $-21504.599 + 281.109149T - 49.9151T\ \ln(T)$

$^{\circ}G_{Fe}^{Liquid} - H_{Fe}^{SER}$

$298.14 < T < 1811$: $12040.17 - 6.55843T - 3.6751551 \times 10^{-21} T^7 + GHSERFE$

$1811 < T < 6000$: $-10839.7 + 291.302T - 46T\ \ln(T)$

$^{\circ}G_{Tb}^{Liquid} - H_{Tb}^{SER}$

$298.14 < T < 1562$: $3945.831 + 29.867521T - 14.252646T\ \ln(T) - 2.0466105 \times 10^{-2} T^2 + 2.17475 \times 10^{-6} T^3 - 160724T^{-1}$

$1562 < T < 3000$: $-13247.649 + 251.16889T - 46.4842T\ \ln(T)$

$800 < T < 3000$: $^{\circ}L_{Dy,Fe}^{Liquid} = -13027^{a}$, $^{\circ}L_{Fe,Tb}^{Liquid} = -37723^{a} + 27^{a}T$

[a]This work.

(2) *Fe_2R (R=Dy or Tb or both):* Two sublattices; sites 0.6667, 0.3333; constituents Fe: Dy, Tb

$800<T<3000$: ${}^{\circ}G_{Fe_2R}-0.3333H^{SER}_{Dy}-0.6667H^{SER}_{Fe}=0.6667\text{GHSERFE}+0.3333\text{GHSERDY}-9974^{a}+0.33^{a}T$

${}^{\circ}G_{Fe_2R}-0.3333H_{Tb}-0.6667H_{Fe}=0.66667\text{GHSERFE}+0.3333\text{GHSERTB}-10041^{a}+3.2^{a}T$

(3) *Fe_3R*: Two sublattices; sites 0.75, 0.25; constituents Fe: Dy, Tb

$800<T<3000$: ${}^{\circ}G_{Fe_3R}-0.25H^{SER}_{Dy}-0.75H^{SER}_{Fe}=0.75\text{GHSERFE}+0.25\text{GHSERDY}-9901^{a}+0.9^{a}T$

${}^{\circ}G_{Fe_3R}-0.25H^{SER}_{Tb}-0.75H^{SER}_{Fe}=0.75\text{GHSERFE}+0.25\text{GHSERTB}-9879^{a}+3.4^{a}T$

(4) *$Fe_{23}R_6$*: Two sublattices; sites 0.793103, 0.206897; constituents Fe: Dy, Tb

$800<T<3000$: ${}^{\circ}G_{Fe_{23}R_6}-0.206897H^{SER}_{Dy}-0.793103H^{SER}_{Fe}=0.793103\text{GHSERFE}+0.206897\text{GHSERDY}-9961^{a}+1.6^{a}T$

${}^{\circ}G_{Fe_{23}R_6}-0.206897H^{SER}_{Tb}-0.793103H^{SER}_{Fe}=0.793103\text{GHSERFE}+0.206897\text{GHSERTB}-9705^{a}+3.5^{a}T$

(5) *$Fe_{17}R_2$*: Two sublattices, sites 0.894737, 0.105263; constituents Fe: Dy, Tb

$800<T<3000$: ${}^{\circ}G_{Fe_{17}R_2}-0.105263H^{SER}_{Dy}-0.894737H^{SER}_{Fe}=0.894737\text{GHSERFE}+0.105263\text{GHSERDY}-9399.5^{a}+2.8^{a}T$

${}^{\circ}G_{Fe_{17}R_2}-0.105263H^{SER}_{Tb}-0.894737H^{SER}_{Fe}=0.894737\text{GHSERFE}+0.105263\text{GHSERTB}-9484^{a}+4.4^{a}T$

Functions

(1) *GHSERFE*

$298.14<T<1811$: $+1225.7+124.134T-23.5143T\ \ln(T)-4.39752\times10^{-3}T^{2}-5.8927\times10^{-8}T^{3}+77359T^{-1}$

$1811<T<6000$: $-25383.581+299.31255T-46T\ \ln(T)+2.29603\times10^{31}T^{-9}$

(2) *GHSERTB*

$298.14<T<600$: $-20842.158+409.309555T-77.5006T\ \ln(T)+8.32265\times10^{-2}T^{2}-2.5672833\times10^{-5}T^{3}+562430T^{-1}$

$600<T<1200$: $-8772.606+102.61162T-25.8659T\ \ln(T)-2.757005\times10^{-3}T^{2}-8.05838\times10^{-7}T^{3}+172355T^{-1}$

$1200<T<1562$: $-7944.942+101.7776T-25.9584T\ \ln(T)-1.676335\times10^{-3}T^{2}-1.067632\times10^{-6}T^{3}$

$1562<T<3000$: $-265240.309+1456.04268T-200.215695T\ \ln(T)+4.1615159\times10^{-2}T^{2}-2.044697\times10^{-6}T^{3}+65043790T^{-1}$

(3) *GHSERDY*

$298.14<T<1000$: $-9129.216+131.734913T-31.3602T\ \ln(T)+6.14295\times10^{-3}T^{2}-2.123617\times10^{-6}T^{3}+31704T^{-1}$

$1000<T<1400$: $46759.596-356.59767T+37.102T\ \ln(T)-2.919595\times10^{-2}T^{2}+9.99035\times10^{-7}T^{3}-8228400T^{-1}$

$1400<T<1659$: $578.987+6.964025T-13.3473T\ \ln(T)-3.82058\times10^{-3}T^{2}-1.466792\times10^{-6}T^{3}$

$1659<T<3000$: $-518996.159+2659.38355T-353.642128T\ \ln(T)+8.0893522\times10^{-2}T^{2}-3.929211\times10^{-6}T^{3}+1.3744487\times10^{8}T^{-1}$